Journal of the European Ceramic Society **17** (1997) 41–47
© 1996 Elsevier Science Limited
Printed in Great Britain. All rights reserved
0955-2219/97/$17.00
PII: S0955-2219(96)00069-6

Cobalt Aluminate Spinel–Mullite Composites Synthesized by Sol–Gel Method

Manuela Sales, Carla Valentín & Javier Alarcón*

Departamento de Química Inorgánica, Facultad de Ciencias Químicas, Universidad de Valencia, 46100 Burjasot (Valencia), Spain

(Received 20 September 1995; revised version received 12 March 1996; accepted 28 March 1996)

Abstract

$CoAl_2O_4$ spinel–mullite composites were prepared by double substitution of Al by Ti and Ni in stoichiometric 3:2 mullite. Gels with compositions $3(Al_{2-2x}Co_xTi_xO_3).2SiO_2$ ($x = 0{\cdot}025$, $0{\cdot}05$ and $0{\cdot}2$) and $3(Al_{2-2x}M_xO_3).2SiO_2$ ($x = 0.05$; $M = Co^{2+}$ or Ti^{4+}) were synthesized by sol–gel techniques. The structure of the gels was investigated by infra-red spectroscopy. Heating gels at 750°C produced an amorphous silicoaluminate network. The reaction sequence was investigated by differential thermal analysis, X-ray diffraction and ultraviolet–visible spectroscopy. All samples crystallized at temperatures lower than 1000°C from the amorphous state. Al–Si spinel and/or $CoAl_2O_4$ were the first crystalline phases detected, which appeared almost simultaneously. This finding indicated the important role played by Co^{2+} and Ti^{4+} in phase development and crystallization kinetics, even for compositions very close to the stoichiometric 3:2. The reaction sequence can understood by assuming that $CoAl_2O_4$ spinel was developed by epitaxial growth on Al–Si spinel. This fact permitted direct control of the final microstructure of the $CoAl_2O_4$ spinel–mullite composite as revealed by scanning and transmission electron microscopies. © 1996 Elsevier Science Limited.

1 Introduction

During the last decade much attention has been paid to mullite composites because they display interesting mechanical, thermal and optical properties. The sol–gel technique has been shown to be a suitable approach for the preparation of novel composites. Both colloidal and polymeric gels have allowed adequate microstructures for the required properties to be developed. Much recent work has focused on the development of mechanical properties;[1,2] however, several reports have demonstrated the usefulness of these techniques for obtaining composites with improved optical properties.[3]

Ceramic pigments are crystalline phases with good optical and chemical properties. Although some ceramic pigments fulfil the requirements of chemical inertness at low temperatures, on increasing temperature they react with glasses. For this reason it is interesting to protect the crystalline phase by developing suitable microstructures, which prevent further chemical attack. This approach has been successful in some pigmenting systems such as Fe_2O_3 and $CdSe_{1-x}S_x$, in which the chromophore phase was encapsulated in a zircon structure. The optical and chemical characteristics of zircon are adequate to allow encapsulated crystalline phases to be developed, because the refractive index and chemical inertness to silicoaluminate glasses are optimum.

Not many other crystalline or amorphous phases that can be developed as encapsulants have been reported. However, silicoaluminates like mullite can be considered for this role because its chemical and optical properties are remarkable. Furthermore, a significant point is the possibility to produce microstructures in which the chromophore particle may be included or protected by the inert crystalline phase during the reaction processes, as was recently evidenced for $NiAl_2O_4$ spinel in mullite.[4]

It was reported that faults produced by pigments were caused by different mechanisms, which range from the degree of pigmenting structure formation to the type and extent of the fluxing used. Cobalt-based pigments are particularly liable to

---

*To whom correspondence should be addressed.

produce faults. It would be interesting, therefore, to increase the stability of that system without affecting its optical properties.[5]

In this paper we report the synthesis and characterization of $CoAl_2O_4$ spinel–mullite composites which withstand high temperatures and are resistant to melted silicoaluminate glazes, so that the former can be used as ceramic pigments at high temperatures. By means of a controlled reaction pathway we thought it would be possible to encapsulate $CoAl_2O_4$ in a mullite matrix, allowing us to reach the above-mentioned requirements. Therefore we examine the crystallization pathway, focusing our attention on the reaction sequence. The microstructural features and optical properties of the samples are discussed as well.

2 Experimental Procedure

2.1 Preparation of gel samples

Gels with compositions $3(Al_{2-2x}Co_xTi_xO_3).2SiO_2$, $x = 0{\cdot}025$, $0{\cdot}050$ and $0{\cdot}200$ (hereafter denoted as samples A, B and C, respectively), and gels with nominal compositions $3(Al_{2-x}M_xO_3).2SiO_2$, with M = Co, Ti and $x = 0.05$ (hereafter referred to as D and E, respectively), were prepared as previously reported for Ni and Ti doping cations. It is to be noted that, except for composition C, all the compositions have Al_2O_3:SiO_2 molar ratios in the range from 2·6:2 to 6·3:2. This Al_2O_3:SiO_2 molar ratio range was claimed previously by Cameron to be the boundaries for continuous solid-solution range on the basis of numerous mullites prepared by a variety of methods.[6] In fact, the stoichiometric phase can be written out as $[Al_2]^{VI}(Si_{2-2x}Al_{2+2x})^{IV}O_{10-x}$, x being in the range from 0·17 to 0·59, which corresponds to the above-mentioned boundaries for continuous solid solution found by Cameron.

Gels were prepared using as starting chemicals tetraethylorthosilicate [TEOS; $Si(OC_2H_5)_4$], aluminium tri-sec-butylate [$Al(OC_4H_9)_3$] and titanium iso-propylate [$Ti(OC_3H_7)_4$], all from Merck & Co. (Darmstadt, Germany), and cobalt chloride from Fluka, by the following procedure. Stoichiometric amounts of $Al(OC_4H_9)_3$ and $Ti(OC_3H_7)_4$ were dissolved in 2-propanol (2-PrOH) by refluxing under nitrogen atmosphere and added to a prehydrolysed TEOS solution which contained the required amount of cobalt chloride. The TEOS:H_2O molar ratio used in prehydrolysis was 1:2, which was performed at 40°C for 20 h. The resultant mixture with a molar ratio TEOS: 2-PrOH = 1:30 was refluxed at 70°C for 5 days, yielding a blue gel.

The gels was first slowly dried by partially sealing a beaker containing the gel with a holed plastic film for several weeks, and then dried in an oven at 120°C. In order to obtain a glass precursor gel dried samples were preheated at 750°C for 3 h. The resulting gel-derived glasses were all violet in colour except for that from sample E, which was white. Glass powder was calcined at temperatures between 900 and 1400°C for 3 and 9 h, and at 1400°C for different holding times.

2.2 Characterization of samples

The chemical and structural evolution of dried gels and crystalline specimens was examined using several techniques.

Infra-red (IR) absorption spectra (model 882, Perkin–Elmer Ltd, Beaconsfield, UK) were obtained in the range 2000–400 cm^{-1} using the KBr pellet method.

Differential thermal analysis (DTA; model 1700, Perkin–Elmer, Norwalk, CT, USA) and thermogravimetric analysis (model 7, Perkin–Elmer, Norwalk, CT, USA) were carried out in air with α-Al_2O_3 liners, using a heating rate of 10°C min^{-1}. Finely powdered alumina was used as reference substance.

X-ray diffraction analysis (model D-500 Siemens, Karlhruhe, Germany) was performed using graphite-monochromated Cu K_α radiation. The diffractometer had two 1° divergence slits, a 1° scatter slit, and a 0·05° receiving slit. Eleven overlap-free reflections between 20° and 70° (2θ) were measured with a scanning speed of 0·12° 2θ min^{-1} using CaF_2 as internal standard. Determination of the lattice constants of mullite was made using LSQC and POWCAL programs.

The microstructure of the as-prepared and thermally treated samples was examined by scanning electron microscopy (SEM) working at 20–30 kV (model S-2500, Hitachi Ltd, Tokyo, Japan). To check the quality of the observation, some of the samples were etched with dilute HF solution for 10 s, and subsequently washed with H_2O. All specimens were coated with gold in an ion-beam coater. The morphology of dried gels and mullite particles was also examined using transmission electron microscopy (model H-800, Hitachi Ltd, Tokyo, Japan) at an accelerating voltage of 200 kV. Samples were prepared by dispersing as-produced and calcined powders in absolute ethyl alcohol and setting dropwise on copper grids that had previously been coated with a holey, thin, carbon film.

Ultraviolet–visible (UV–Vis) spectra of the specimens (model Lambda 9, Perkin–Elmer, Norwalk, CT, USA) were acquired using the diffuse reflectance technique in order to examine the local structure of the Co^{2+} cation.

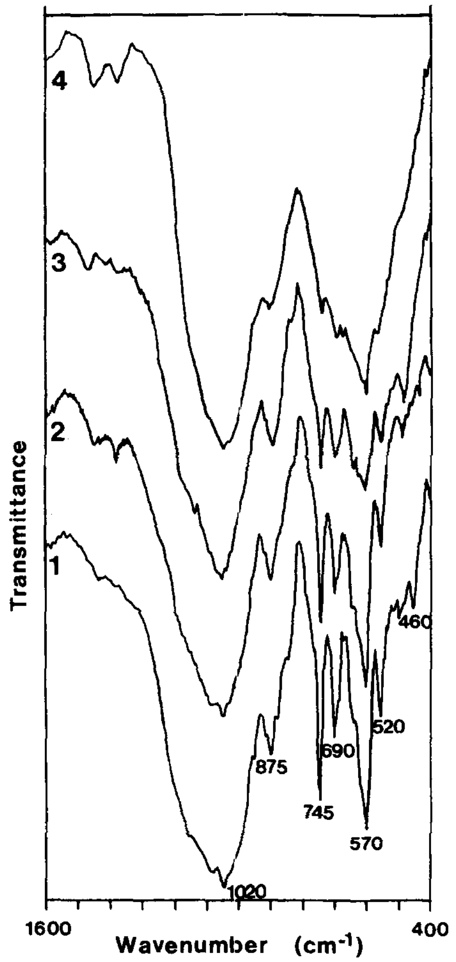

Fig. 1. IR absorption spectra of dried gels: (1) sample D, (2) sample A, (3) sample B and (4) sample C.

3 Results and Discussion

3.1 Gel synthesis and structural development of gel samples up to 750°C

As-prepared gels with different compositions were transparent and seemingly homogeneous. As expected, the blue colour became more and more intense as the Co content was raised and the Ti-containing gels were colourless. IR spectra of dried gels at 120°C are given in Fig. 1. The characteristic bands around 875 and 1020 cm^{-1} associated with the Si–O–Al bond are observed.[7,8] These bands indicate the formation of a silicoaluminate network in the amorphous dried gels. The small absorption band at 940 cm^{-1} is attributed to the Si–O–Ti stretching vibration,[9] which implies the network former function of the Ti^{4+} ion in the gels. Differences in band intensity as a function of titanium content are not detectable owing to the small amount of titanium in the samples.

In addition to those mentioned above, other bands are observed in the range from 500 to 800 cm^{-1} which are associated with Al–O and Ti–O bonds, Al in tetrahedral and octahedral coordination and Ti in octahedral coordination.

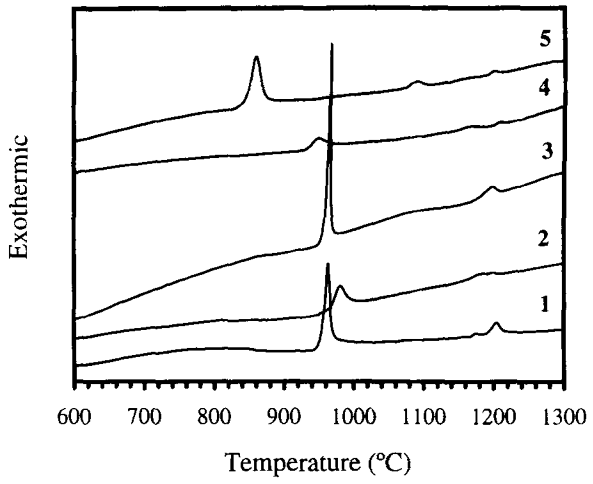

Fig. 2. DTA curves of gels heat-treated at 750°C for 3 h: (1) sample D, (2) sample E, (3) sample A, (4) sample B and (5) sample C.

3.2 Crystallization of samples

DTA heating curves of samples preheated at 750°C are depicted in Fig. 2. Broadly speaking, these DTA curves are quite similar to those previously reported for Ti/Ni-mullite samples.[10] As can be seen, the exothermic effects occur at lower temperatures upon increasing x, i.e. the amount of substitution. A summary of crystalline phases detected after switching off the furnace at specific temperatures and cooling down is given in Table 1.

The X-ray diffraction patterns of samples after the first exothermic effect allow us to associate the effect to the crystallization of Al–Si spinel (also referred to as γ-Al_2O_3 in the literature) and/or $CoAl_2O_4$ spinel. As is well known, however, the gels heated past the sharp, first exotherm show a diffraction pattern of poorly crystalline Al–Si spinel. That fact gives rise to some difficulty in determining whether $CoAl_2O_4$ spinel is present or not along with Al–Si spinel at the first stage of crystallization.

In contrast with the success in determining the formation of $NiAl_2O_4$ spinel with respect to Al–Si spinel by UV–Vis spectroscopy in Ni and Ti-containing mullites,[10] in this case with Ti and Co it has not been so clearly evidenced that formation of $CoAl_2O_4$ spinel takes place after Al–Si spinel. UV–Vis spectra and X-ray diffraction patterns of samples heated at several temperatures and holding times, before and after the exothermic effect, are depicted in Fig. 3. As can be seen, the characteristic spectrum of $CoAl_2O_4$ spinel is detected just when crystallization of Al–Si spinel occurs. It can be assumed that $CoAl_2O_4$ crystallizes after Al–Si spinel, which is understood if the former crystalline phase grows epitaxially on the latter. This behaviour, previously reported by us in the Ni–Ti mullite system, is observed even in samples with lower x value, that is for compositions very close to the stoichiometric 3:2 mullite.

Table 1. Crystalline phases related to DTA exothermic peaks

Sample	*After 1st exothermic peak*	*Before 2nd exothermic peak*	*After 2nd exothermic peak*	*After 3rd exothermic peak*	*After DTA curve (~1400°C)*
A[a]	1015°C Al/Si spinel + amorphous		1200°C Mullite + $CoAl_2O_4$ (traces)		1400°C Mullite + $CoAl_2O_4$ (traces)
B	960°C Al/Si spinel + amorphous		1200°C Mullite + $CoAl_2O_4$		1330°C Mullite + $CoAl_2O_4$
C[b]	910°C Al/Si spinel + amorphous	1075°C Mullite + $CoAl_2O_4$ + rutile (traces)	1200°C Mullite + $CoAl_2O_4$ + rutile		1400°C Mullite + $CoAl_2O_4$ + $CoTiO_3$ (traces)
D	1000°C Al/Si spinel + amorphous	1130°C Al/Si spinel + $CoAl_2O_4$ + amorphous	1200°C Mullite + $CoAl_2O_4$	1250°C Mullite + $CoAl_2O_4$	1350°C Mullite + $CoAl_2O_4$
E	990°C Al/Si spinel + amorphous	1125°C Al/Si spinel + mullite + amorphous	1180°C Mullite		1365°C Mullite

[a] Only two exothermic peaks are observed.
[b] Four exothermic peaks are observed.

First, it should be noted that the 3:2 mullite follows a different crystallization path.[11-13] It crystallizes directly and fully to mullite with a sharp and intense exothermic effect in DTA curves. However, with the introduction of as little as 1·40 and 1·31 wt% TiO_2 and CoO, respectively, only Al–Si spinel forms during a similar but less intense exotherm without detecting any mullite. Spinel formation around 1000°C has been attributed to heterogeneous alumina–silica mixing. Thus, experimental conditions can lead to segregation of alumina and silica even in alkoxide-derived gels. Previously we have found spinel as well as mullite after the exothermic effect at 1000°C in undoped Al_2O_3-rich mullites prepared from alkoxides. This fact can result from the great difference in hydrolysis rates of silicon and aluminium alkoxides, which gives rise to segregation of alumina–silica. Even though partially hydrolysed TEOS is used, a small amount of crystallized spinel is observed. It is noteworthy, however, that in our samples and with such small amounts of dopants as included for the specimen with $x = 0.025$, the thermal evolution is so strikingly different. The apparent discrepancy can be explained by taking into account that thermally produced changes depend on both kinetic and thermodynamic factors. Thus, if the growth kinetics are favourable, even a metastable phase is predicted thermodynamically if this phase is nucleated prior to a stable phase. In the present case, it is suggested that both cations (cobalt and titanium) facilitate the formation of alumina aggregates, i.e. segregation of alumina, which first transform to γ-Al_2O_3 and then to Al–Si spinel.

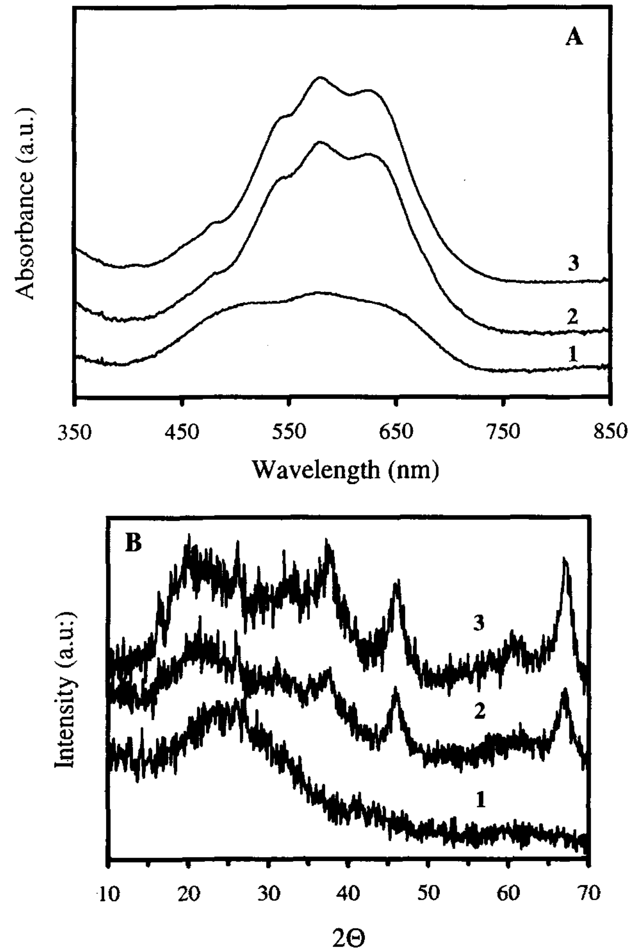

Fig. 3. (A) UV–V spectra and (B) X-ray diffraction patterns of sample A fired at low temperatures: (1) 750°C/3 h; (2) 995°C/0 h; and (3) 995°C/1 h.

The mullite formation in the sample with the smaller amount of Co/Ti occurs without displaying any apparent thermal effect in the DTA curve. For specimens with a higher amount of Co and/or Ti, two exothermic effects are associated with

Table 2. Lattice parameters for doped mullites heated at 1400°C for 96 h (sample C heated for 8 h)

Sample	*a (Å)*	*b (Å)*	*c (Å)*
A	7·5495 ± 0·0009	7·6923 ± 0·0011	2·8868 ± 0·0004
B	7·5531 ± 0·0012	7·6971 ± 0·0014	2·8899 ± 0·0006
C	7·5578 ± 0·0012	7·7009 ± 0·0014	2·8918 ± 0·0005
D	7·5432 ± 0·0007	7·6901 ± 0·0008	2·8840 ± 0·0003
E	7·5482 ± 0·0012	7·6986 ± 0·0014	2·8896 ± 0·0006
JCPDS 15-776	7·5456	7·6898	2·8842

mullite formation; except for the sample with $x = 0.2$, in which a thermal effect is not observed. In addition, three exothermic and one endothermic effects are detected, the former being associated with rutile, cristobalite and $CoTiO_3$ respectively, and the latter with partial melting.

X-ray diffraction patterns of samples heat-treated at several temperatures and holding times are generally consistent with the above path. For Co-containing samples calcined at 1400°C for 96 h, only mullite and $CoAl_2O_4$ spinel are detected. A small content of $CoTiO_3$, however, is also detected for samples with a larger amount of Co/Ti cations.

3.3 Lattice parameters and microstructure of samples

Lattice parameters for samples doped with either Co or Ti and codoped with both are displayed in Table 2. Likewise, and for comparison purposes, reported values corresponding to the stoichiometric 3:2 mullite have been included.[11] The unsubstituted reference mullite was prepared following a similar procedure to that used for the doped samples. As can be seen, the lattice parameters show a slight increase with increasing amount of dopants. This fact can be understood if it is assumed that the increasing lattice parameter is caused by the replacement of aluminium by titanium and/or nickel, even though a decrease will be produced in mullites becoming richer in SiO_2. As is well known, the structure of mullite may be thought of as being derived from the disordered sillimanite $SiO_2.Al_2O_3$, by the exchange of Al^{3+} for Si^{4+} and the removal of oxygen anions.[14] Thus, the stoichiometric phase may be written out as $[Al_2]^{VI}(Si_{2-2x}Al_{2+2x})^{IV}O_{10-x}$ and it corresponds to a crystalline phase with variable composition, i.e. a solid solution.

Fig. 4. SEM micrograph of sample A fired at 1400°C/96 h; bar = 1 μm.

Fig. 5. SEM micrograph of sample B fired at 1400°C/96 h; bar = 1 μm.

From the increasing lattice parameters it seems evident that the amount of dopants incorporated into the structure is increased. However, the actual mechanism of solid-solution formation is difficult to establish since there are several processes taking place simultaneously, such as aluminium replacement by titanium and cobalt, and silicon replacement by aluminium. A more complete study of solid solution ranges and mechanisms is currently in progress.

Secondary electron images of samples obtained by SEM are displayed in Figs 4, 5 and 6, and reveal no homogeneity in size and shape of particles. Three main types of particle may be distinguished: the first type is formed by large, elongated, prismatic particles displaying irregular surface. Small polyhedric particles with edge ≤ 2 μm belong to the second type. Also, small elongated particles with smooth surfaces can be distinguished. These particle features indicate that possibly the Al_2O_3:SiO_2 molar ratio is different for

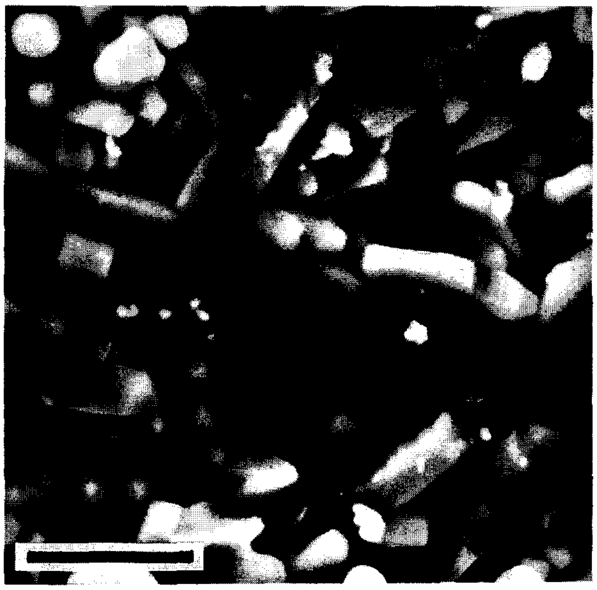

Fig. 6. SEM micrograph of sample D fired at 1400°C/96 h; bar = 1 μm.

each one, but in all cases the particles are richer in SiO_2 than 3:2. The occurrence of elongated particles may be explained by the formation of mullites rich in SiO_2 that have been grown in the presence of a liquid phase.[15,16]

Backscattered electron images of polished specimens are shown in Figs 7, 8 and 9. A matrix of dark contrast, which is composed mainly of Al and Si but also of Ti and Co, is detected. Some particles with lighter contrast are also seen inside the matrix, these displaying two kinds of composition: ones containing Al and Co, and the others (less numerous) having Co and Ti as main constituents with some Al. This result is consistent with that obtained by X-ray diffraction, where both $CoAl_2O_4$ and $CoTiO_3$ were detected in the sample with the higher amount of dopant.

3.4 UV–Vis spectroscopy of samples

UV–Vis spectra of samples fired at 1400°C for 96 h are displayed in Fig. 10. It is well known that Co^{2+} is a cation with electronic configuration d^7, which in tetrahedral and octahedral coordination presents three bands allowed by spin and others that may be assigned to transitions forbidden by spin.[17] From crystallochemistry point of view $CoAl_2O_4$ spinel is normal,[18] i.e. Co^{2+} is placed mainly in tetrahedral coordination. The full spectrum displayed fits very well with some previously described by us for $CoAl_2O_4$.[19] However, for higher amount of dopants and at higher temperatures, strong absorption is displayed at higher energies, which is a specific characteristic of $CoTiO_3$.

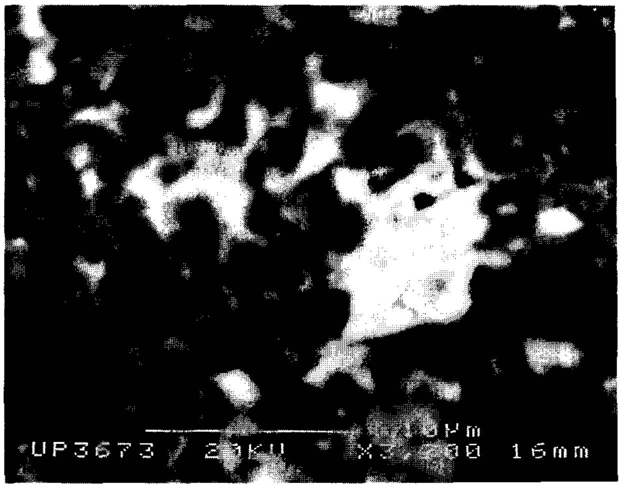

Fig. 8. Backscattered SEM micrograph of sample C fired at 1400°C/96 h.

4 Conclusions

$CoAl_2O_4$ spinel—mullite composite precursors were prepared by sol–gel techniques. Monophasic gels with nominal compositions $3(Al_{2-2x}Co_x-Ti_xO_3).2SiO_2$, $0{\cdot}025 \leq x \leq 0.2$, and $3(Al_{2-x}M_xO_3).2SiO_2$, $x = 0.05$ and $M = Co^{2+}$ or Ti^{4+}, were formed by hydrolysis and condensation of mixtures

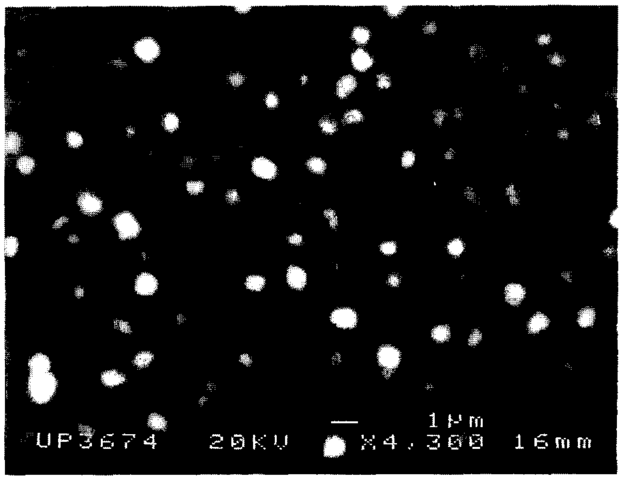

Fig. 7. Backscattered SEM micrograph of sample A fired at 1400°C/ 96 h.

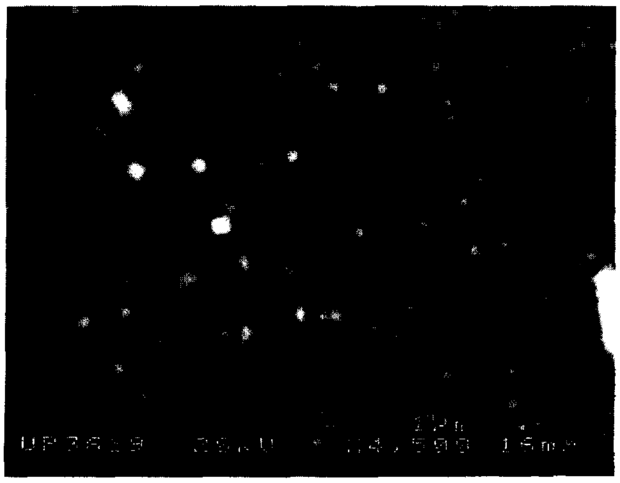

Fig. 9. Backscattered SEM micrograph of sample D fired at 1400°C/96 h.

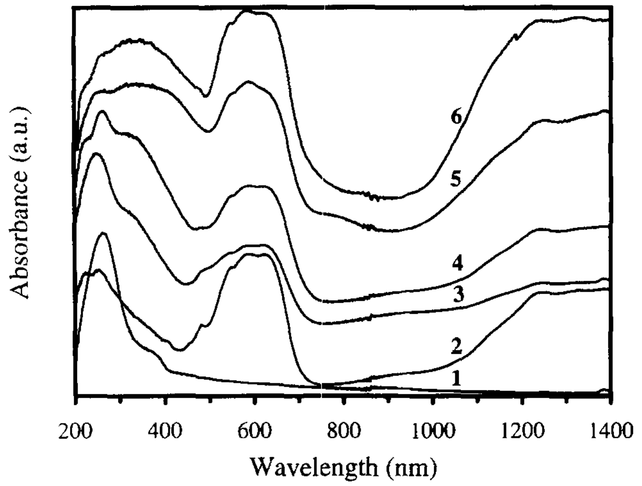

Fig. 10. UV–V spectra of samples fired at 1400°C/96 h ($CoAl_2O_4$ fired at 1100°C/2 h): (1) sample E, (2) sample D, (3) sample A, (4) sample B, (5) sample C and (6) $CoAl_2O_4$.

of aluminium, silicon and titanium alkoxides and cobalt chloride.

Al–Si spinel was the first crystalline phase detected below 1000°C. The crystallization temperature was dependent on the nominal composition of specimens. Almost simultaneously $CoAl_2O_4$ spinel was detected, but the reaction sequence was not so clearly evidenced as in $NiAl_2O_4$ spinel–mullite systems. However, results were also consistent with an epitaxial growth mechanism of $CoAl_2O_4$ spinel onto Al–Si spinel phase.

Secondary electron images for specimens also displayed the presence of mullite prismatic particles growing directionally and suggesting the presence of a liquid phase. The occurrence of particles with different composition to the matrix (or aggregates) was also confirmed by backscattered electron images. These inclusions were identified by energy dispersive X-ray analysis as $CoAl_2O_4$.

The UV–Vis spectra of composites were observed to fit that of $CoAl_2O_4$ in the visible region of the electromagnetic spectrum.

Acknowledgement

Financial support for the present work was provided by CICYT (Project MAT92-0423).

References

1. Ismail, M. G. M. U., Tsunatori, H. & Nakai, Z., Preparation of mullite cordierite composite powders by the sol–gel method: its characteristics and sintering. *J. Am. Ceram. Soc.*, **73** (1990) 537–543.
2. Yuan, Q. M., Tan, J. Q., Shen, J. Y., Zhu, X. H. & Yang, Z. F., Processing and microstructure of mullite zirconia composites prepared from sol–gel powders. *J. Am. Ceram Soc.*, **69** (1986) 268–269.
3. Sales, M., Valentín, C. & Alarcón, J., Spinel–mullite compositions with optical properties. Presented at *8th International Workshop on Glasses and Ceramics from Gels*, Faro, Portugal, 18–22 September 1995.
4. Sales, M. & Alarcón, J., Solid solutions with mullite structure in SiO_2–Al_2O_3–TiO_2–MO (M^{2+} = Co, Ni) systems. *Bol. Soc. Esp. Cerám. Vidr.*, **34** (1995) 81–86.
5. Airey, A. C., Pigment development. *Br. Ceram. Trans. J.*, **86** (1987) 138–142.
6. Cameron, W. E., Mullite a substituted alumina. *Am. Mineral.*, **62** (1977) 747–755.
7. Nogami, M., Ogawa, S. & Nagasaka, K., Preparation of cordierite glass by the sol–gel process. *J. Mater. Sci.*, **24** (1989) 4339–4342.
8. Pancrazi, F. Phalippou, J., Sorrentino, F. & Zarzycki, J., Preparation of gels in the CaO–Al_2O_3–SiO_2 system from metal alkoxides. *J. Non-Cryst. Solids*, **63** (1984) 81–93.
9. Congshen, Z., Lisong, H., Fuxi, G. & Zhonghong, J., Low temperature synthesis of ZrO_2–TiO_2–SiO_2-glasses from $Zr(NO_3)_4.5H_2O$, $Si(OC_2H_5)_4$ and $Ti(OC_4H_9)_4$ by the sol–gel method. *J. Non-Cryst. Solids*, **63** (1984) 105–115.
10. Sales, M., Valentín, C. & Alarcón, J., Reaction sequence in the preparation of $NiAl_2O_4$ spinel–mullite composites by sol–gel. *J. Am. Ceram. Soc.*, to be published.
11. Sales, M. & Alarcón, J., Structural evolution of mullite gels. *Bol. Soc. Esp. Cerám. Vidr.*, **33** (1994) 273–278.
12. Li, D. X. & Thomson, W. J., Mullite formation kinetics of a single-phase gel. *J. Am. Ceram. Soc.*, **73**[4] (1990) 964–969.
13. Okada, K., Hoshi, Y. & Otsuka, N., Formation reaction of mullite from SiO_2–Al_2O_3 xerogels. *J. Mater. Sci. Lett.*, **5**[12] (1986) 1316–1318.
14. Angel, R. A. & Prewitt, C. T., Crystal structure of mullite: a re-examination of the average structure. *Am. Mineral.*, **71** (1986) 1476–1482.
15. Li, D. X. & Thomson, W. J., Mullite formation from non stoichiometric diphasic precursors. *J. Am. Ceram. Soc.*, **74** (1991) 2382–2387.
16. Mizuno, M., Preparation of highly pure fine mullite powders. *J. Am. Ceram. Soc.*, **72** (1989) 377–382.
17. Schmitz-Dumont, O., Spectrochemical investigation on the structural characteristics of oxidic lattices containing transition metals. *Bull. Soc. Chim.*, (1965) 1099–1105.
18. West, A. R., Some factors which influence crystal structures. In *Solid State Chemistry and Its Applications*, John Wiley & Sons Ltd, UK, 1984, pp. 264–317.
19. Alarcón, J., Escribano, P. & Marin, R. M., Co(II) based ceramic pigments. *Br. Ceram. Trans. J.*, **84** (1985) 170–172.